Sensitivity Analysis

Oliwer Sliczniuk[a,*], Pekka Oinas[a]

[a]*Aalto University, School of Chemical Engineering, Espoo, 02150, Finland*

ARTICLE INFO

ABSTRACT

The article presents a comprehensive study on the supercritical fluid extraction of essential oil from chamomile flowers, focusing on model dynamics and applying a distributed-parameter model to describe the fluid-solid extraction process. By employing the concept of quasi-one-dimensional flow, the study simplifies the spatial dimensions of the extraction process, ensuring uniform flow across any cross-section while allowing for variations in the area available for the fluid phase. The physical properties of the solvent are estimated using the Peng-Robinson equation of state. The model was validated under multiple constant operating conditions: $30-40°C$, $100-200$ bar, and $3.33-6.67\cdot10^{-5}$ kg/s. The model dynamic is investigated by analysing how sensitive the model output is to model parameters. In this work, the local sensitivity analysis is introduced and used to examine the influence of infinitely small changes in the pressure on the model's state space and the extraction yield.

1. Introduction

This study investigates the extraction of essential oil from chamomile flowers (Matricaria chamomilla L.) via supercritical fluid extraction techniques and the modelling of this process. Chamomile is a medicinal herb widely cultivated in southern and eastern Europe in countries such as Germany, Hungary, France and Russia. It can be found outside Europe, for instance in Brazil as discussed by Singh et al. [1]. This plant is distinguished by its hollow, bright gold cones, housing disc or tubular florets and surrounded by about fifteen white ray or ligulate florets. Chamomile has been used for its medicinal benefits, serving as an anti-inflammatory, antioxidant, mild astringent, and healing remedy. Aqueous extract of chamomile is widely used to calm nerves and mitigate anxiety, hysteria, nightmares, insomnia and other sleep-related conditions, according to Srivastava [2]. Orav et al. [3] reported that oil yields from dried chamomile samples ranged from 0.7 to 6.7 mL/kg. The highest yields of essential oil, between 6.1 and 6.7 mL/kg, were derived from chamomile sourced from Latvia and Ukraine. In comparison, chamomile from Armenia exhibited a lower oil content of 0.7 mL/kg.

Evaluating the economic viability of the process is essential when choosing a suitable technology for essential oil extraction. Traditional methods, such as distillation and organic solvent extraction, are commonly employed but have drawbacks. Distillation, for example, involves high temperatures that can lead to the thermal degradation of heat-sensitive compounds. This limitation has led to the increased popularity of alternative techniques such as supercritical fluid extraction. Supercritical carbon dioxide is appealing thanks to its distinctive properties: it is inflammable, non-toxic and non-corrosive. Supercritical fluids can exhibit both gas- and liquid-like properties, allowing for adjustable dissolving power through changes in operating conditions.

The literature offers various mathematical models to describe the extraction of valuable compounds from biomass. Selecting a process model is case-to-case dependent and requires analysis of each model's specific assumptions about mass transfer and thermodynamic equilibrium.

The model proposed by Reverchon et al. [4] is called the hot ball model, as it is based on an analogy to heat transfer and describes an extraction process from solid particles. This model assumes that particles contain low quantities of solute and that solubility is not a limiting factor.

The Broken-and-Intact Cell model, proposed by Sovova [5], assumes that external surfaces of particles are mechanically disrupted, allowing the solvent access to the solute in the broken cells. In contrast, the solute in intact cells remains less accessible due to higher mass transfer resistance.

Reverchon [6] formulated a fluid-solid extraction model where the solute is treated as a single component, governed by internal mass transfer resistance and omitting the effects of external mass transfer, axial dispersion and variations in fluid density and flow rate throughout the bed.

This work builds upon the linear kinetic model suggested by Reverchon [6], deriving fundamental governing equations to develop a comprehensive model for the chamomile oil extraction process. This model aims for control-oriented simplicity, assuming a semi-continuous operation within a cylindrical vessel. The process involves a supercritical solvent being pumped through a fixed bed of finely chopped biomass to extract the solute, followed by separation of the solvent and solute in a flush drum to collect the extract. Parameters such as pressure (P), feed flow rate (F_{in}) and inlet temperature (T_{in}) are adjustable and measurable, while the outlet temperature (T_{out}) and the amount of product at the outlet can only be monitored. Figure 1 presents a simplified process flow diagram.

This study aims to analyse the influence of changes in operating conditions on the supercritical extraction model described in article 1. The relation between input and output is obtained by applying a sensitivity analysis. Sensitivity analysis examines the impact of varying inputs or model parameters on the system's output. The aim is to understand

---

*Corresponding author

✉ oliwer.sliczniuk@aalto.fi (O. Sliczniuk)

ORCID(s): 0000-0003-2593-5956 (O. Sliczniuk); 0000-0002-0183-5558 (P. Oinas)
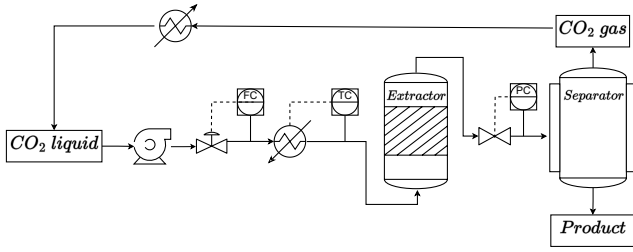
Figure 1: Process flow diagram

and allocate the source of uncertainty in the output to the corresponding inputs or parameters. There are many sensitivity analysis methods, which include but are not limited to those listed below:

- One-at-a-time method

- Derivative-based local methods

- Variance-based methods

Different supercritical extraction models were analysed using sensitivity analysis. Fiori et al. [7], performed the sensitivity calculations by varying the parameters within their confidence interval and observing how the model results changed. This allows to evaluate the effect of the uncertainties on model predictions. The sensitivity analysis revealed that the particle diameter and the internal mass transfer coefficient are the most influential factors in the extraction process. The effect of changing operating conditions was also investigated, underlining how solvent flow rate and seed milling affect extraction.

In the work of Santos et al. [8], a diffusive model for the semi-continuous, isothermal, and isobaric extraction process is analysed by a parametric sensitivity analysis using a factorial design in two levels. The parametric sensitivity analysis was carried out by applying disturbances of 10% in the values of nominal values of velocity, particle diameter, and initial concentration in the solid and liquid phases. The authors concluded that it is necessary to determine the optimum particle diameter and manipulate the solvent superficial velocity to control the process.

Hatami and Ciftci [9] used a one-factor-at-a-time sensitivity analysis and employed two distinct strategies to conduct their analysis: the first strategy involved applying an equal fluctuation to all technical and economic parameters, while the second strategy utilised real ranges for fluctuating these parameters. The authors found that the most influential factors on NPV include the price of the extract, the interest rate, the dynamic time of SFE, and the project lifetime. Moreover, in this study tried to determine rhe upper and lower bounds for technical and economic factors, utilizing pertinent literature data.

Poletto and Reverchon [10] provided a general dimensionless model for the supercritical vegetable and essential oils extraction process and applied a sensitivity analysis. They found that a dimensionless partition coefficient and

a dimensionless characteristic time are the most influential parameters of the extraction process. The sensitivity calculations were performed by varying the parameters and analysing the model response.

2. Materials and methods

2.1. Governing equations

Following the work of Anderson [11], the governing equations for a quasi-one-dimensional flow were derived. A quasi-one-dimensional flow refers to a fluid flow scenario assuming that the flow properties are uniformly distributed across any cross-section. This simplification is typically applied when the flow channel's cross-sectional area changes, such as through irregular shapes or partial filling of an extractor. According to this assumption, velocity and other flow properties change solely in the flow direction.

As discussed by Anderson [12], all flows are compressible, but some of them can be treated as incompressible when the Mach number is smaller than 0.3. This assumption leads to the incompressible condition: $\nabla \cdot u = 0$, which is valid for constant density (strict incompressible) or varying density flow. The assumption allows for removing acoustic waves and large perturbations in density and/or temperature. In the 1-D case, the incompressibility condition becomes $\frac{du}{dz} = 0$, so the fluid velocity is constant.

The set of quasi-one-dimensional governing equations in Cartesian coordinates is described by Equations 1 - 3:

$$\frac{\partial \left(\rho_f A_f \right)}{\partial t} + \frac{\partial \left(\rho_f A_f v \right)}{\partial z} = 0 \tag{1}$$

$$\frac{\partial \left(\rho_f v A_f \right)}{\partial t} + \frac{\partial \left(\rho_f A_f v^2 \right)}{\partial z} = -A_f \frac{\partial P}{\partial z} \tag{2}$$

$$\frac{\partial \left(\rho_f e A_f \right)}{\partial t} + \frac{\partial \left(\rho_f A_f v e \right)}{\partial z} = -P \frac{\left(A_f v \right)}{\partial z} + \frac{\partial}{\partial z} \left(k \frac{\partial T}{\partial z} \right) \tag{3}$$

where ρ_f is the density of the fluid, A_f is the function which describes a change in the cross-section, v is the velocity, P is the total pressure, e is the internal energy of the fluid, t is time and z is the spatial direction.

2.2. Extraction model

2.2.1. Continuity equation

The previously derived quasi-one-dimensional continuity equation (Equation 1) is redefined by incorporating the function $A_f = A\phi$. This modification distinguishes constant and varying terms, where the varying term accounts for changes in the cross-sectional area available for the fluid. Equation 4 shows the modified continuity equation:

$$\frac{\partial (\rho_f \phi)}{\partial t} + \frac{\partial (\rho_f v A \phi)}{\partial z} = 0 \tag{4}$$

where A is the total cross-section of the extractor and ϕ describes porosity along the extractor.

Assuming that the mass flow rate is constant in time, the temporal derivative becomes the mass flux F, and the spatial derivative can be integrated along z as

$$\int \frac{\partial (\rho_f v A \phi)}{\partial z} dz = F \rightarrow F = \rho_f v A \phi \tag{5}$$

To simplify the system dynamics, it is assumed that F is a control variable and affects the whole system instantaneously (due to $\nabla \cdot u = 0$), which allows finding the velocity profile that satisfies mass continuity based on F, ϕ and ρ_f:

$$v = \frac{F}{\rho_f A \phi} \qquad (6)$$

Similarly, superficial velocity may be introduced:

$$u = v\phi = \frac{F}{\rho_f A} \qquad (7)$$

The fluid density ρ_f can be obtained from an equation of state (Appendix **??**) if the temperature and thermodynamic pressure are known along z. Variation in fluid density may occur due to pressure or inlet temperature changes. In a non-isothermal case, in Equations 6 and 7 ρ_f is considered the average fluid density along the extraction column.

2.2.2. Mass balance for the fluid phase

Equation 8 describes the movement of the solute in the system, which is constrained to the axial direction due to the quasi-one-dimensional assumption. Given that the solute concentration in the solvent is negligible, the fluid phase is described as pseudo-homogeneous, with properties identical to those of the solvent itself. It is also assumed that the thermodynamic pressure remains constant throughout the device. The analysis further simplifies the flow dynamics by disregarding the boundary layer near the extractor's inner wall. This leads to a uniform velocity profile across any cross-section perpendicular to the axial direction. Thus, the mass balance equation includes convection, diffusion and kinetic terms representing the fluid phase behaviour:

$$\frac{\partial c_f}{\partial t} + \frac{1}{\phi}\frac{\partial \left(c_f u\right)}{\partial z} = \frac{1-\phi}{\phi}r_e + \frac{1}{\phi}\frac{\partial}{\partial z}\left(D_e^M \frac{\partial c_f}{\partial z}\right) \qquad (8)$$

where c_f represents the solute concentration in the fluid phase, r_e is the mass transfer kinetic term and D_e^M is the axial diffusion coefficient.

2.2.3. Mass balance for the solid phase

As given by Equation 9, the solid phase is considered stationary, without convection and diffusion terms in the mass balance equation. Therefore, the only significant term in this equation is the kinetic term of Equation 10, which connects the solid and fluid phases. For simplicity, the extract is represented by a single pseudo-component:

$$\frac{\partial c_s}{\partial t} = \underbrace{r_e}_{\text{Kinetics}} \qquad (9)$$

2.2.4. Kinetic term

As the solvent flows through the bed, CO_2 molecules diffuse into the pores and adsorb on the particle surface to form an external fluid film around the solid particles due to the solvent-solid matrix interactions. The dissolved solute diffuses from the particle's core through the solid-fluid interface, the pore and the film into the bulk. Figure 2 shows the mass transfer mechanism, where the mean solute concentration in the solid phase is denoted as c_s, and the equilibrium

concentrations at the solid-fluid interface are denoted as c_s^* and c_p^* for the solid and fluid phases, respectively. The concentration of the solutes in the fluid phase in the centre of the pore is denoted as c_p. As the solute diffuses through the pore, its concentration changes and reaches c_{pf} at the pore opening. Then, the solute diffuses through the film around the particle and reaches bulk concentration c_f. The two-film theory describes the solid-fluid interface inside the pore. The overall mass transfer coefficient can be determined from the relationship between the solute concentration in one phase and its equilibrium concentration.
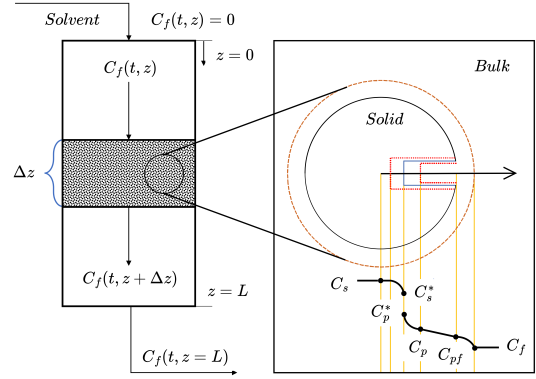

Figure 2: Mass transfer mechanism.

Bulley et al. [13] suggest a process where the driving force for extraction is given by the difference between the concentration of the solute in the bulk, c_f, and in the centre of the pore, c_p^*. The concentration c_p^* is in equilibrium with c_s according to the equilibrium relationship. The rate of extraction is thus $r_e\left(c_f - c_p^*(c_s)\right)$. In contrast, Reverchon [6] proposes a driving force given by the difference between c_s and c_p^*. Concentration c_p^* is determined by the equilibrium relationship with c_f and the extraction rate given by Equation 10:

$$r_e = \frac{D_i}{\mu l^2}\left(c_s - c_p^*\right) \qquad (10)$$

where μ is sphericity, l a characteristic dimension of particles that can be defined as $l = r/3$, r is the mean particle radius, ρ_s is the solid density, D_i corresponds to the overall diffusion coefficient and c_P^* is the concentration at the solid-fluid interface (which according to the internal resistance model is supposed to be at equilibrium with the fluid phase).

According to Bulley et al. [13], a linear equilibrium relationship (Equation 11) can be used to find the equilibrium concentration of the solute in the fluid phase c_f^* based on the concentration of the solute in the solid phase c_s:

$$c_f^* = k_p c_s \qquad (11)$$

The volumetric partition coefficient k_p acts as an equilibrium constant between the solute concentration in one phase and the corresponding equilibrium concentration at the solid-fluid interphase. According to Spiro and Kandiah

[14], k_p can be expressed through the mass partition coefficient k_m:

$$k_m = \frac{k_p \rho_s}{\rho_f} \tag{12}$$

According to Reverchon [6], the kinetic term becomes

$$r_e = -\frac{D_i}{\mu l^2}\left(c_s - \frac{\rho_s c_f}{k_m \rho_f}\right) \tag{13}$$

2.2.5. Uneven solute's distribution in the solid phase

Following the idea of the Broken-and-Intact Cell (BIC) model (Sovova [15]), the internal diffusion coefficient D_i is considered to be a product of the reference value of D_i^R and the exponential decay function γ, as given by Equation 14:

$$D_i = D_i^R \gamma(c_s) = D_i^R \exp\left(\Upsilon\left(1 - \frac{c_s}{c_{s0}}\right)\right) \tag{14}$$

where Υ describes the curvature of the decay function. Equation 15 describes the final form of the kinetic term:

$$r_e = -\frac{D_i^R \gamma}{\mu l^2}\left(c_s - \frac{\rho_s c_f}{k_m \rho_f}\right) \tag{15}$$

The γ function limits the solute's availability in the solid phase. Similarly to the BIC model, the solute is assumed to be contained in the cells, some of which are open because the cell walls were broken by grinding, with the rest remaining intact. The diffusion of the solute from a particle's core takes more time than the diffusion of the solute close to the outer surface. The same idea can be represented by the decaying internal diffusion coefficient, where the decreasing term is a function of the solute concentration in the solid.

Alternatively, the decay function γ can be interpreted by referring to the Shrinking Core model presented by Goto et al. [16], where the particle radius changes as the amount of solute in the solid phase decreases. As the particle size decreases due to dissolution, the diffusion path increases, which makes the diffusion slower and reduces the value of the diffusion coefficient. This analogy can be applied to Equation 14 to justify the application of a varying diffusion coefficient.

2.2.6. Heat balance

The heat balance equation describe the evolution of the internal energy in the system and it is given by Equation 16

$$\frac{\partial\left(\rho_f h A_f\right)}{\partial t} = -\frac{\partial\left(\rho_f h A_f v\right)}{\partial z} + \frac{\partial\left(P A_f\right)}{\partial t} + \frac{\partial}{\partial z}\left(k\frac{\partial T}{\partial z}\right) \tag{16}$$

The main advantage of this formulation is the presence of term $\partial P/\partial t$, which directly affects the system through the change of thermodynamic pressure (which is a control variable).

If the value of enthalpy h is known from the time evolution of the energy equation, and pressure P is known from measurement, then the temperature T can be reconstructed based on the departure function. The departure function is a mathematical function that characterizes the deviation of a thermodynamic property (enthalpy, entropy, and internal energy) of a real substance from that of an ideal gas at the same temperature and pressure. The departure function is defined as the difference between the value of a thermodynamic property for a real fluid and the corresponding value for an ideal gas at the same temperature and pressure. They are computed by integrating a function that depends on the equation of state and its derivatives. As presented by Gmehling et al. [17], for the Peng-Robinson equation of state, the enthalpy can be defined by Equation 17.

$$h - h^{id} = RT\left[T_r(Z-1) - 2.078(1+\kappa)\sqrt{\alpha(T)}\ln\left(\frac{Z+\left(1+\sqrt{2}\right)B}{Z+\left(1-\sqrt{2}\right)B}\right)\right] \tag{17}$$

Equation 17 requires an reference sate, which is assumed to be $T_{ref} = 298.15$[K] and $P_{ref} = 1.01325$[bar].

A root-finder can be used to find a value of temperature, which minimizes the difference between the value of enthalpy coming from the heat balance and the departure functions. The root fining procedure to repeated at every time step to find a local temperature along spatial direction z.

$$\min_T\left(\underbrace{h(t,x)}_{\text{Heat balance}} - \underbrace{h\left(T,P,\rho_f(T,P)\right)}_{\text{Departure function}}\right)^2 \tag{18}$$

2.2.7. Pressure term

The pressure term in the energy equation, given by Equation 16, describes the change of the thermodynamic pressure with respect to time. As explained in Chapters 2.1, at Low-Mach number conditions, the thermodynamic pressure is nearly constant in space due to the small pressure wave propagation that occurs at the speed of sound. Under such conditions, the term $\partial P/\partial t$ can be approximated by a difference equation, which describes the pressure change in the whole system. The pressure (P) in the system is considered a state variable, while the pressure in the new time-step (P_{in}) is considered a control variable.

$$\frac{\partial P(t)}{\partial t} \approx \frac{P_{in}(t) - P(t)}{\Delta t} \tag{19}$$

Such a simplified equation allows for instantaneous pressure change in the system but does not consider a gradual pressure build-up and the effects of pressure losses. In a real system, the dynamics of pressure change would depend on a pump used in an extraction system and a back-pressure regulator used to control an outlet valve.

2.2.8. Extraction yield

The process yield is calculated according to Equation 20 as presented by Sovova et al. [18]. The measurement equation evaluates the solute's mass at the extraction unit outlet and sums it up. The integral form of the measurement (Equation 20) can be transformed into the differential form (Equation 21) and augmented with the process model.

$$y = \int_{t_0}^{t_f} \frac{F}{\rho_f} c_f\bigg|_{z=L} dt \tag{20}$$

$$\frac{dy}{dt} = \frac{F}{\rho_f} c_f\bigg|_{z=L} \tag{21}$$

2.2.9. Initial and boundary conditions

It is assumed that the solvent is free of solute at the beginning of the process $c_{f0} = 0$, that all the solid particles have the same initial solute content c_{s0}, and that the system is isothermal, hence the initial state is h_0. The fluid at the inlet is considered not to contain any solute. The initial and boundary conditions are defined as follows:

$$c_f(t = 0, z) = 0 \qquad c_s(t = 0, z) = c_{s0} \qquad h(t = 0, z) = h_0$$

$$c_f(t, z = 0) = 0 \qquad h(t, z = 0) = h_{in}(t) \qquad \frac{\partial c_f(t, z = L)}{\partial x} = 0$$

$$\frac{\partial h(t, z = L)}{\partial x} = 0 \qquad c_s(t, z = \{0, L\}) = 0 \qquad y(0) = 0 \quad P(0) = P_0$$

2.2.10. Discretization methods

The method of lines is used to transform the process model equations into a set of ODEs denoted as $G(x; \Theta)$. The backward finite difference is used to approximate the first-order derivative, while the central difference scheme approximates the second-order derivative z direction. The length of the fixed bed is divided into N_z, i.e. equally distributed points in the z direction. The state-space model after discretization is denoted as x and defined as follows:

$$\dot{x}(t) = \frac{dx}{dt} = \begin{bmatrix} \frac{dc_{f,1}(t)}{dt} \\ \vdots \\ \frac{dc_{f,N_z}(t)}{dt} \\ \hline \frac{dc_{s,1}(t)}{dt} \\ \vdots \\ \frac{dc_{s,N_z}(t)}{dt} \\ \hline \frac{dh_1(t)}{dt} \\ \vdots \\ \frac{dh_{N_z}(t)}{dt} \\ \hline \frac{dP(t)}{dt} \\ \hline \frac{dy(t)}{dt} \end{bmatrix} = \underbrace{\begin{bmatrix} G_1\left(c_f, c_s, h; \Theta\right) \\ \vdots \\ G_{N_z}\left(c_f, c_s, h; \Theta\right) \\ \hline G_{N_z+1}\left(c_f, c_s, h; \Theta\right) \\ \vdots \\ G_{2N_z}\left(c_f, c_s, h; \Theta\right) \\ \hline G_{2N_z+1}\left(c_f, c_s, h; \Theta\right) \\ \vdots \\ G_{3N_z}\left(c_f, c_s, h; \Theta\right) \\ \hline G_{3N_z+1}\left(c_f, c_s, h; \Theta\right) \\ \hline G_{3N_z+2}\left(c_f, c_s, h; \Theta\right) \end{bmatrix}}_{G(x;\Theta)}$$

where $x \in \mathbb{R}^{N_x = 3N_z + 2}$ and $\Theta \in \mathbb{R}^{N_\Theta = N_\theta + N_u}$, N_θ is the number of parameters, N_u is the number of control variables.

For a derivative to be conservative, it must form a telescoping series. In other words, only the boundary terms should remain after adding all terms coming from the discretization over a grid, and the artificial interior points should be cancelled out. Discretization is applied to the conservative form of the model to ensure mass conservation.

2.3. Sensitivity Analysis

Local derivative-based methods involve taking the total derivative of the state vector x with respect to parameters p, where p is a subset of the parameter space θ. The set of derivatives, known as sensitivity equations, is integrated simultaneously with the process model. The sensitivity analysis shows how responsive the solution is for changes in the parameter p. As discussed by Dickinson and Gelinas [19], the sensitivity analysis can be used to determine the influence of the uncertainty on the solution of the original system. A sensitivity analysis can be used to distinguish sensitive parameters from insensitive ones, which might be helpful for model reduction. Finally, from a control engineering point of view, the sensitivity analysis allows sorting the control variables with respect to the level of effort required to change the model's output.

Following the work of Maly and Petzold [20], the sensitivity analysis equations($\dot{Z}$) can be defined as follow:

$$Z(x(t); p) = \frac{dx(t)}{dp} \tag{22}$$

The new system of equations can be obtained by taking derivatives of Z with respect to time t and applying the chain rule.

$$\dot{Z}(x(t); p) = \frac{dZ(x(t); p)}{dt} = \frac{d}{dt}\left(\frac{dx(t)}{dp}\right) = \frac{d}{dp}\left(\frac{dx(t)}{dt}\right) = \frac{dG(x(t); p)}{dp} \tag{23}$$

The sensitivity equation can be obtained by applying the definition of the total derivative to Equation 23.

$$\frac{dG(x(t); p)}{dp} = \underbrace{\frac{\partial G(x(t); p)}{\partial x(t)}}_{J_x(x(t); p)} \underbrace{\frac{\partial x(t)}{\partial p}}_{S(x(t); p)} + \underbrace{\frac{\partial G(x(t); p)}{\partial p}}_{J_p(x(t); p)} \tag{24}$$

Equation 24 is solved simultaneously with the process model and consists of three terms: Jacobian $J_x(x(t); p)$, sensitivity matrix $S(x(t); p)$ and Jacobian $J_p(x(t); p)$. The Jacobian $J_x(x(t); p)$ represents the matrix of equations of size $N_x \times N_x$, where each equation $J_x(n_x, n_x)$ is the derivative of $G_{n_x}(x(t); p)$ with respect to the state variable x_{n_p}.

$$J_x(x(t); p) = \begin{pmatrix} \frac{\partial G_1(x(t); p)}{\partial x_1(t)} & \frac{\partial G_1(x(t); p)}{\partial x_2(t)} & \cdots & \frac{\partial G_1(x(t); p)}{\partial x_{N_x}(t)} \\ \frac{\partial G_2(x(t); p)}{\partial x_1(t)} & \frac{\partial G_2(x(t); p)}{\partial x_2(t)} & \cdots & \frac{\partial G_2(x(t); p)}{\partial x_{N_x}(t)} \\ \vdots & \vdots & \ddots & \vdots \\ \frac{\partial G_{N_x}(x(t); p)}{\partial x_1(t)} & \frac{\partial G_{N_x}(x(t); p)}{\partial x_2(t)} & \cdots & \frac{\partial G_{N_x}(x(t); p)}{\partial x_{N_x}(t)} \end{pmatrix} \tag{25}$$

The sensitivity matrix $S(x(t); p)$ represents the matrix of equations of size $N_x \times N_p$, where each subequation $S(n_x, n_p)$ is the derivative of the state variable x_{n_x} with respect to the parameter p_{n_p}. Matrix $J_x(x(t); p)$ and $S(x(t); p)$ describe indirect influence of p_{n_p} on the model output.

$$S(x(t); p) = \begin{pmatrix} \frac{\partial x_1(t)}{\partial p_1} & \frac{\partial x_1(t)}{dp_2} & \cdots & \frac{dx_1(t)}{\partial p_{N_p}} \\ \frac{\partial x_2(t)}{\partial p_1} & \frac{\partial x_2(t)}{dp_2} & \cdots & \frac{dx_2(t)}{\partial p_{N_p}} \\ \vdots & \vdots & \ddots & \vdots \\ \frac{\partial x_{N_x}(t)}{\partial p_1} & \frac{\partial x_{N_x}(t)}{dp_2} & \cdots & \frac{\partial x_{N_x}(t)}{\partial p_{N_p}} \end{pmatrix} \tag{26}$$

The Jacobian $J_p(x(t); p)$ represents the matrix of equations of size $N_x \times N_p$, where each subequation $J_p(n_x, n_p)$ is the partial derivative of the process model equation F_{n_x} with respect to the parameter p_{n_p}. $J_p(n_x, n_p)$ defines direct effect of p_{n_p} on the model output.

$$J_p(x(t); p) = \begin{pmatrix} \dfrac{\partial G_1(x(t); p)}{\partial p_1} & \dfrac{\partial G_1(x(t); p)}{\partial p_2} & \cdots & \dfrac{\partial G_1(x(t); p)}{\partial p_{N_p}} \\ \dfrac{\partial G_2(x(t); p)}{\partial p_1} & \dfrac{\partial G_2(x(t); p)}{\partial p_2} & \cdots & \dfrac{\partial G_2(x(t); p)}{\partial p_{N_p}} \\ \vdots & \vdots & \ddots & \vdots \\ \dfrac{\partial G_{N_x}(x(t); p)}{\partial p_1} & \dfrac{\partial G_{N_x}(x(t); p)}{\partial p_2} & \cdots & \dfrac{\partial G_{N_x}(x(t); p)}{\partial p_{N_p}} \end{pmatrix} \tag{27}$$

The combined system containing the original set of equations $G(x(t); p)$ and sensitivity equations can be formulated as $\mathbf{G}(x(t); p)$. The size of $\mathbf{G}(x(t); p)$ is equal to $N_s = N_x(N_p + 1)$.

$$\mathbf{G}(x(t); p) = \begin{bmatrix} G(x(t); p) \\ J_x(x(t); p)S(x(t); p) + J_p(x(t); p) \end{bmatrix} \tag{28}$$

The initial conditions are described as

$$\mathbf{G}(x(t_0); p) = \begin{bmatrix} x(t_0), & \dfrac{dx(t_0)}{dp_1}, & \cdots, & \dfrac{dx(t_0)}{dp_{N_p}} \end{bmatrix}^\top = \tag{29}$$

$$= \begin{bmatrix} x_0, & 0, & \cdots, & 0 \end{bmatrix}^\top \tag{30}$$

The sensitivity analysis of the output function can be performed with respect to parameters p. The output function $g(x(t))$ returns $y(t)$. By taking a total derivative of $y(t)$ with respect to p, the new sensitivity equation can be found.

$$\frac{dy(t)}{dp} = \frac{dg(x(t))}{dp} = \frac{\partial g(x(t))}{\partial x(t)} \frac{\partial x(t)}{\partial p} + \frac{\partial g(x(t))}{\partial p} \tag{31}$$

3. Results

This work investigates the influence of pressure change on the state space and the extraction yield. The process model and parameters have been discussed in article 1. The process model was calibrated on the set of experiments obtained at different operating conditions, $30 - 40°C$, $100 - 200$ bar, and $3.33 - 6.67 \cdot 10^{-5}$ kg/s. The sensitivity analysis has been performed assuming that the system operates at $35°C$, 150 bar and $5 \cdot 10^{-5}$ kg/s.

As discussed in Chapter 2.1, a small pressure wave propagates at the speed of sound relative to the flow. If the flow velocity is relatively low, all pressure changes are hydrodynamic (resulting from velocity motion) rather than thermodynamic. The Low Mach-number assumption leads to instant propagation of the thermodynamic pressure throughout the system. A single pressure value can be considered for the entire system, as all changes occur simultaneously throughout the device. A step-function shown in Figure 3 illustrates the pressure change in the extractor.

The model is built such that the pressure change first affects $\frac{dP}{dt}$, and in the next time step, the energy balance through $\frac{\partial(P(t)A_f)}{\partial t}$, leading to the step change along the whole
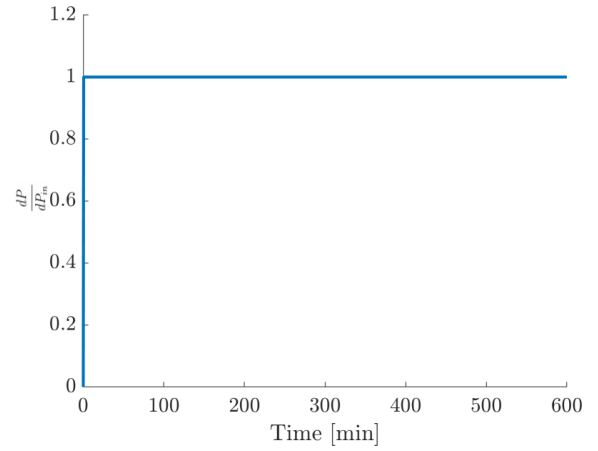
Figure 3: The effect of P_{in} change on P in the system

system as presented in Figure 4. The energy balance response becomes noticeable, as well as the change in the physical properties of the solvent. The uniform response across the entire extraction column length, represented by the homogeneously dark red colour, indicates that the whole system experiences an immediate and uniform change in enthalpy density in response to pressure changes.

The pressure change affects the fluid's temperature inside the computational domain, but boundary values are subject to constraints specified at the extremes of that domain. Applying the Dirichlet boundary conditions assumes a fixed temperature value at the inlet, which can lead to a thermal gradient propagating along the system. In contrast, Neumann boundary conditions would dictate the heat flux at the boundaries. In this work, the Neumann boundary conditions equal to zero were applied to ensure that the temperatures at the inlet, the outlet, and the middle of the extractor are the same all the time.
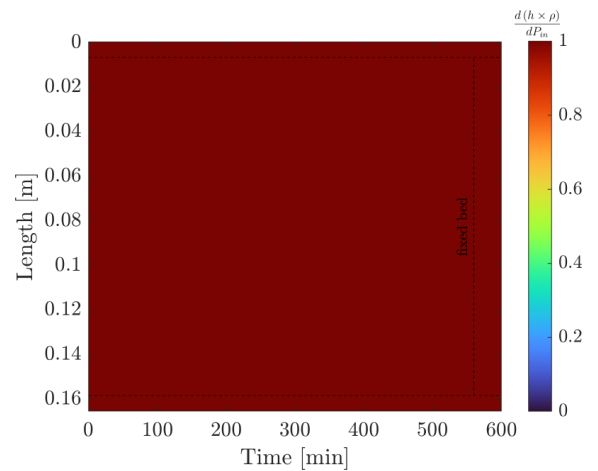
Figure 4: The effect of P_{in} change on $(h \times \rho)$ in the system

Figure 5 shows the sensitivity of the solute concentration in the solid phase with respect to pressure change along a fixed bed in a supercritical fluid extraction process. As

discussed in Chapter 2.2.1, the velocity of a fluid is inversely proportional to its density, which suggests that the pressure increase decreases the velocity. This leads to an extended residence time, ergo, a longer interaction between the solute and the solvent. Initially, the extraction process is in the kinetically-controlled regime, where the concentration gradient is high, and the limiting factor is the solute solubility. As discussed in (article 1), the system is considered to be far from saturation, which can explain the low system response at the beginning of the process. The system response becomes more evident when the concentration gradient starts diminishing, and the extraction switches from the kinetic-controlled to the diffusion-controlled regime. The negative sign can be interpreted as a faster solute loss from the solid phase, which corresponds to enhanced mass transfer. Over time, the amount of solute becomes a limiting factor, and the pressure change has a lower effect on the system. Eventually, the sensitivities approach zero asymptotically when the solute is exhausted from the solid bed.
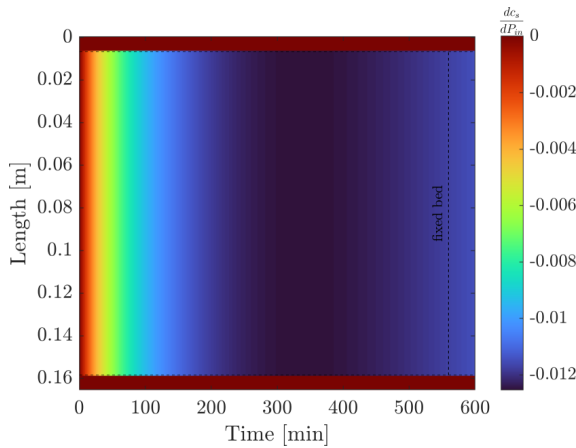

Figure 5: The effect of P_{in} change on C_s

Figure 6 shows how sensitive is the solute concentration in the fluid phase to the pressure change. Although the pressure increase enhances the mass transfer, the system response is initially low, which reflects the idle period discussed above. Later, the sensitivities increase due to faster solute loss from the solid phase, which indicates that more solute is transported to the fluid phase. When the amount of solute in the solid phase becomes a limiting factor, the extraction rate slows down, sensitivities decline asymptotic towards zero, and the impact of the pressure change decreases. The advection causes the sensitivities to move along the system analogously to the solute in the fluid phase.

Figure 7 illustrates how sensitive the extraction yield is to the pressure change. Initially, the sensitivity curve stays almost flat, suggesting a latency in the system's response to pressure changes. Due to the decreased velocity of the fluid, the solute reaches the extractor's outlet later, which causes minor negative sensitivities to appear. The process continues, and the sensitivity curve increases rapidly when the solute reaches the extractor's outlet. The positive yield
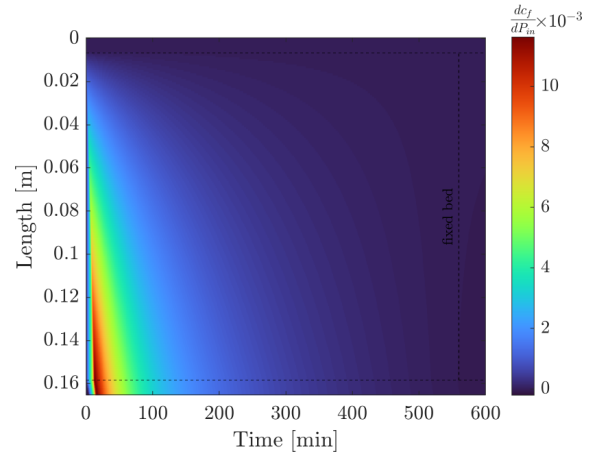

Figure 6: The effect of P_{in} change on C_f

sensitivity indicates improved process efficiency, which is directly related to enhanced mass transfer. The peak in $\frac{dy}{dP_{in}}$ reflects when the deviation from the original system is the largest. Beyond the peak, the sensitivity declines and converges towards zero. The concentration gradient becomes a limiting factor, and the enhanced mass transfer no longer plays a dominant role compared to the original system.
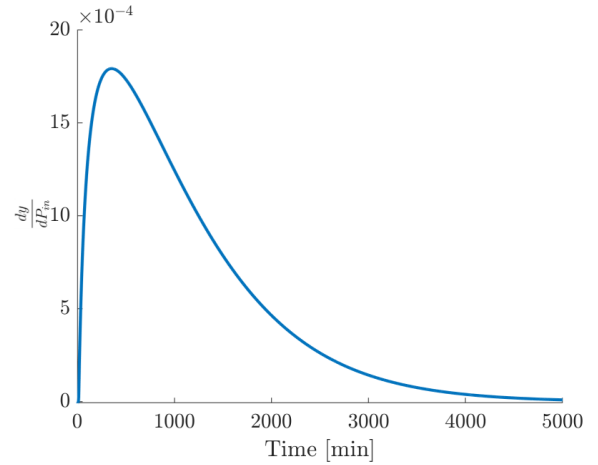

Figure 7: The effect of P_{in} change on $y(t)$

4. Conclusions

Sensitivity analysis is a tool to understand how parameters affect a model's output. In the case of dynamical systems, local sensitivity analysis provides a time series describing how that dependency evolves. The presented formulation involves derivative-based local sensitivity analysis of the model solution with respect to selected parameters and controls. The local sensitivity analysis techniques consider only a small region of parameter space, and the conclusions derived from such an analysis are limited to local conditions unless the discussed system is a linear model. The sensitivity equations can be obtained in various ways. This

work implemented the automatic differentiation technique to get the sensitivity equations, which evaluate the effect of pressure increase on the supercritical extraction model. At given operating conditions ($35°C$, 150 bar and $5 \cdot 10^{-5}$ kg/s), the step change of pressure enhance the mass transfer, which leads to faster loss of solute from solid particles and consequently to negative sensitivities in the solid phase. An analogous response is visible in the fluid phase, where the concentration of solute increases and is visible as positive sensitivities. As more solute is transported to the fluid phase, the extraction yield is improved and characterised by positive sensitivities. Local sensitivity analysis can provide valuable information about process modelling, experiment design, or model reduction by identifying which parameters are influential and how these influence changes over time.

References

[1] Ompal Singh, Zakia Khanam, Neelam Misra, and Manoj Kumar Srivastava. Chamomile (matricaria chamomilla l.): An overview. Pharmacognosy Reviews, 5(9):82, 2011. ISSN 0973-7847. doi: 10.4103/0973-7847.79103.

[2] Janmejai Srivastava. Extraction, characterization, stability and biological activity of flavonoids isolated from chamomile flowers. Molecular and Cellular Pharmacology, 1(3):138–147, August 2009. ISSN 1938-1247. doi: 10.4255/mcpharmacol.09.18.

[3] Anne Orav, Ain Raal, and Elmar Arak. Content and composition of the essential oil ofchamomilla recutita(l.) rauschert from some european countries. Natural Product Research, 24(1):48–55, January 2010. ISSN 1478-6427. doi: 10.1080/14786410802560690.

[4] Ernesto Reverchon, Giorgio Donsi, and Libero Sesti Osseo. Modeling of supercritical fluid extraction from herbaceous matrices. Industrial & Engineering Chemistry Research, 32(11):2721–2726, nov 1993. doi: 10.1021/ie00023a039.

[5] H. Sovova. Rate of the vegetable oil extraction with supercritical co2. modelling of extraction curves. Chemical Engineering Science, 49(3):409–414, 1994. doi: 10.1016/0009-2509(94)87012-8.

[6] E. Reverchon. Mathematical modeling of supercritical extraction of sage oil. AIChE Journal, 42(6):1765–1771, June 1996. ISSN 1547-5905. doi: 10.1002/aic.690420627.

[7] L. Fiori, D. Calcagno, and P. Costa. Sensitivity analysis and operative conditions of a supercritical fluid extractor. The Journal of Supercritical Fluids, 41(1):31–42, may 2007. doi: 10.1016/j.supflu.2006.09.005.

[8] M.M. Santos, E.A. Boss, and R. Maciel Filho. Supercritical extraction of oleaginous: parametric sensitivity analysis. Brazilian Journal of Chemical Engineering, 17(47):713–720, December 2000. ISSN 0104-6632. doi: 10.1590/s0104-66322000000400035.

[9] Tahmasb Hatami and Ozan N. Ciftci. Techno-economic sensitivity assessment for supercritical co2 extraction of lycopene from tomato processing waste. The Journal of Supercritical Fluids, 204:106109, January 2024. ISSN 0896-8446. doi: 10.1016/j.supflu.2023.106109.

[10] Massimo Poletto and Ernesto Reverchon. Comparison of models for supercritical fluid extraction of seed and essential oils in relation to the mass-transfer rate. Industrial & Engineering Chemistry Research, 35(10):3680–3686, January 1996. ISSN 1520-5045. doi: 10.1021/ie9600093.

[11] John D. Anderson. Computational fluid dynamics the basic with applications. McGraw-Hill, 1995. ISBN 9780071132107.

[12] J. D. Jr Anderson. Fundamentals of Aerodynamics. McGraw-Hill Education, 2023. ISBN 9781264151929.

[13] N. R. Bulley, M. Fattori, A. Meisen, and L. Moyls. Supercritical fluid extraction of vegetable oil seeds. Journal of the American Oil Chemists' Society, 61(8):1362–1365, aug 1984. doi: 10.1007/bf02542243.

[14] M. Spiro and M. Kandiah. Extraction of ginger rhizome: partition constants and other equilibrium properties in organic solvents and in supercritical carbon dioxide. International Journal of Food Science & Technology, 25(5):566–575, jun 2007. doi: 10.1111/j.1365-2621.1990.tb01116.x.

[15] Helena Sovova. Broken-and-intact cell model for supercritical fluid extraction: Its origin and limits. The Journal of Supercritical Fluids, 129:3–8, nov 2017. doi: 10.1016/j.supflu.2017.02.014.

[16] Motonobu Goto, Bhupesh C. Roy, and Tsutomu Hirose. Shrinking-core leaching model for supercritical-fluid extraction. The Journal of Supercritical Fluids, 9(2):128–133, jun 1996. doi: 10.1016/s0896-8446(96)90009-1.

[17] Jürgen Gmehling, Michael Kleiber, Bärbel Kolbe, and Jürgen Rarey. Chemical Thermodynamics for Process Simulation. Wiley, mar 2019. doi: 10.1002/9783527809479.

[18] H. Sovova, R. Komers, J. Kucuera, and J. Jezu. Supercritical carbon dioxide extraction of caraway essential oil. Chemical Engineering Science, 49(15):2499–2505, aug 1994. doi: 10.1016/0009-2509(94)e0058-x.

[19] Robert P. Dickinson and Robert J. Gelinas. Sensitivity analysis of ordinary differential equation systems—a direct method. Journal of Computational Physics, 21(2):123–143, jun 1976. doi: 10.1016/0021-9991(76)90007-3.

[20] Timothy Maly and Linda R. Petzold. Numerical methods and software for sensitivity analysis of differential-algebraic systems. Applied Numerical Mathematics, 20(1-2):57–79, feb 1996. doi: 10.1016/0168-9274(95)00117-4.

[21] Ding-Yu Peng and Donald B. Robinson. A new two-constant equation of state. Industrial & Engineering Chemistry Fundamentals, 15(1):59–64, feb 1976. doi: 10.1021/i160057a011.